IMA Journal of Applied Mathematics Advance Access published June 8, 2012

IMA J Appl Math (2012) 77(3): 391-398

IMA Journal of Applied Mathematics (2012) Page 1 of 8
doi:10.1093/imamat/hxs026

Coherent structures in transitional plane Couette flow

PAUL MANNEVILLE
LadHyX, École polytechnique, Palaiseau, France
paul.manneville@polytechnique.edu

[Received on 26 September 2011; accepted on 1 February 2012]

We briefly review the recent work on turbulent coherent structures in the transition *to* and *from* turbulence in wall-bounded flows, with special emphasis on the plane Couette flow for which these structures self-organize to form a pattern of bands alternately laminar and turbulent.

Keywords: coherent structures; patterns; transition to turbulence.

1. Context

In applied mathematics coherent structures, e.g. solitary waves, are most often understood as special solutions to partial differential equations that can further be turned into homo/heteroclinic solutions to ordinary differential equations by an appropriate change of frame. On the other hand, in turbulence studies they present themselves as some sort of large-scale organized motion that is persistent in time and correlated in space on a small-scale turbulent background. The transition to turbulence in some wall-bounded flows offers an interesting mixture of these two viewpoints.

The Reynolds number R is the usual control parameter for flows. It is defined as $R = UL/\nu$, where U is the scale of velocity fluctuations over some relevant length scale L, and ν is the kinematic velocity of the fluid. In contrast with shear flows displaying inflection points in their velocity profiles (mixing layers, jets and wakes, etc.), flows controlled by the presence of walls (pipe or channel flows, boundary layers, etc.) are usually protected from inertial instabilities of the Kelvin–Helmholtz type that develop at low R and experience an abrupt transition to turbulence at moderate R, well below the threshold for viscous instabilities of the Tollmien–Schlichting type that are possibly effective at high R only. For a review, see Manneville (2010, Chapter 7).

The two most emblematic cases are the flow in a pipe of circular cross section under a given pressure gradient or mass flux, and the plane Couette flow between two parallel counter-translating plates. Both are known to be linearly stable for all R, while becoming turbulent at moderately large R. The transition is marked by an important hysteresis and characterized by the coexistence of laminar and turbulent flows in some finite-width range of R. Below a lower threshold that we denote by $R_{\rm g}$, 'g' for global, the turbulence is only *transient*. Above a second threshold, denoted by us as $R_{\rm t}$, an essentially uniform or *featureless* turbulent flow prevails, and hence the subscript 't'.

As far as pattern formation is concerned, the pipe flow is a basically one-dimensional system. Its case has recently been clarified (see, e.g. Avila *et al.*, 2011; Barkley, 2011). Turbulent coherent structures travelling in laminar flow called *puffs* have finite lifetimes but, when R is large enough, can split and contaminate the rest of the flow. The Reynolds number being conventionally defined as $R = UD/\nu$ with U the mean fluid velocity and D the pipe diameter, below $R_{\rm g} \approx 2{,}040$ the decay probability is larger than the probability of splitting so that, in the long term, the flow is laminar. On the contrary, above that limit splitting wins and an intermittent mingling of laminar and turbulent flows can persist indefinitely.

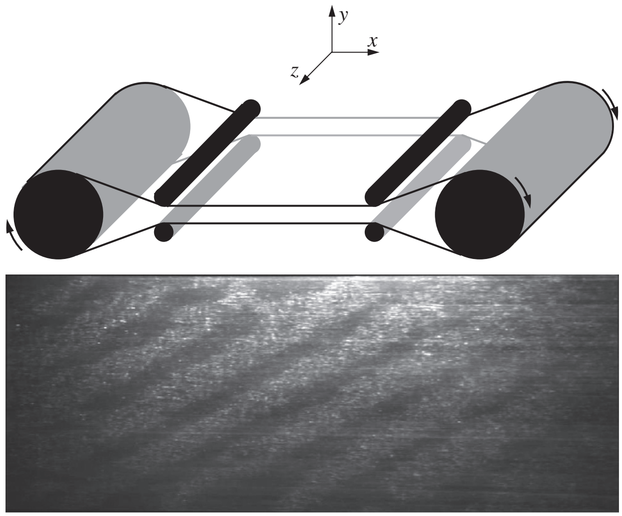

FIG. 1. Top: typical setup used to study plane Couette flow. Bottom: turbulent band pattern observed at $R = 358$, courtesy A. Prigent, Saclay.

Threshold R_t for featureless turbulence has not been localized with the same degree of confidence but for $R \approx 2600$ puffs become *slugs*, domains filled with small-scale turbulence of ever increasing length due to upstream fronts getting slower and downstream edges getting faster as illustrated and studied quantitatively by Duguet *et al.* (2010a). Despite some still finite probability of local and temporary collapse of turbulence, this particular value of R could be identified with R_t since essentially uniform turbulence is expected at the end of a sufficiently long pipe. One, however, still has to push R beyond $\sim$2,900 to obtain uniform turbulence most of the time. Of course, all this holds provided that turbulence is *triggered* by appropriate finite-amplitude perturbations since laminar flow can easily be maintained up to much higher values, 10000 or more, in well-designed experiments with a low level of background turbulence.

Let us now consider the plane Couette flow (Fig. 1, top) which, on the one hand, is free from complications arising from the overall downstream mass flux but, on the other hand, is effectively two-dimensional, while with symmetries allowing relevant perturbations to stay at rest in the laboratory frame. In a series of experiments, researchers at Saclay (for a review, see Prigent & Dauchot, 2005) have determined the main characteristics of the bifurcation diagram. Here, the Reynolds number is defined as $R = Uh/\nu$, where $\pm U$ are the speeds of the moving plates and $2h$ the distance between them. Below $R_g \approx 325$, finite-lifetime turbulence is observed in the form of *spots* as shown by Bottin *et al.* (1998). Above $R_t \approx 410$, *featureless turbulence* prevails. Between these two values, at a large enough aspect ratio (in-plane dimensions compared with gap) a steady regime of turbulence made of oblique bands, alternately laminar and turbulent, has been observed by Prigent *et al.* (2003) (see Fig. 1, bottom). They have also shown that the transition to featureless turbulence is continuous in the sense that the modulation of the turbulence intensity decreases progressively as R_t is approached from below. On the other hand, near R_g bands break down into spots which, having finite lifetime, decay to a laminar flow.

Some understanding of the processes sustaining turbulence has been obtained from the careful interpretation of numerical simulations within the conceptual framework of the so-called *minimal flow unit* (MFU). The MFU introduced by Jiménez & Moin (1991) is a computational domain extending over the full wall-normal dimension of the considered system with periodic in-plane (streamwise and spanwise) boundary conditions set at a distance just necessary to maintain chaotic dynamics at the moderate values of R of interest. The mechanism proposed by Hamilton *et al.* (1995) involves *streamwise vortices* inducing *streaks* that break down to regenerate the vortices. For the plane Couette flow, Waleffe (2003) showed that this mechanism reaches some sort of optimal efficiency in an MFU of size $\ell_x \times 2h \times \ell_z$ with $\ell_x \approx 12.8h$ and $\ell_z \approx 4.2h$.

Coherence of the flow at the corresponding scales supports an analysis of the dynamics in terms of dynamical systems. Resting on exact solutions of Navier–Stoke equations (see, e.g. Gibson *et al.*, 2009), unstable periodic orbits and homoclinic tangles, this approach has led to an interpretation of turbulence in terms of *chaotic transients*, as reviewed by Eckhardt *et al.* (2008), the frontier between laminar flow and turbulence being associated to *edge states* and manifolds attached to them; see Schneider *et al.* (2008) for the plane Couette flow.

Studies at the scale of the MFU are, however, by essence, unable to account for the most striking phenomenon of transitional wall-bounded flows, namely the coexistence of laminar flow and turbulence in physical space. This coexistence is attested at much larger scales in spatially extended systems rather than in systems that are actually confined by in-plane periodic boundary conditions at distances of the order of a few h. Experiments at Saclay have indeed been performed in systems of size ($L_x \times L_z$) ranging from ($250h \times 100h$) in Bottin *et al.* (1998) to ($700h \times 300h$) in Prigent *et al.* (2003). Laminar-turbulent patterns, when observed in the largest systems, had roughly constant streamwise wavelengths $\lambda_x \approx 110h$ and spanwise wavelengths ranging from $\lambda_z \sim 50h$ near R_t to $\sim 80h$ near R_g.

The first numerical study dedicated to the problem of bands has been performed by Barkley & Tuckerman (2005a). They used a computational domain tilted with respect to the streamwise direction, transversally long ($\gtrsim 40h$) but longitudinally short ($10h$). This trick was very efficient in reproducing the bands at limited computational cost, the price to pay being just a breaking of symmetry imposed in advance between the two possible orientations allowed by the geometry. Later, the bands were obtained in wide domains of sizes comparable to experimental ones by Duguet *et al.* (2010b) in close agreement with laboratory findings. The latter simulations were extremely demanding from a computational standpoint. By means of wall-normal under-resolved numerical simulations understood as a consistent and systematic modelling strategy to be illustrated below, Manneville & Rolland (2010) showed that the mechanism at the origin of bands was remarkably robust, provided that the resolution be sufficient for rendering large-scale streamwise correlations. According to Philip & Manneville (2011), the same reason explains that, mimicking streamwise coherence decay on a longer scale than the nominal size of their oblique domain, Barkley and Tuckerman could obtain realistic bands despite periodic boundary conditions at MFU distances in the longitudinal direction, whereas the bands are not present in an MFU-long strictly spanwise-aligned computational domain.

2. Some results

Experiments have posed interesting pattern formation problems in the transitional range of the plane Couette flow. It may thus seem valuable to perform simulations in the *thermodynamic limit* of large aspect-ratio systems, while avoiding the ab initio restriction of Barkley & Tuckerman (2005b), i.e. by taking $L_{x,z} \gg \lambda_{x,z} \gg \ell_{x,z}$ for long enough durations so as to reach a statistical equilibrium. Such simulations are still computationally too much demanding in the fully resolved case (Duguet *et al.*, 2010b), which suggests resorting to controlled under-resolution as introduced above. The study has been done using ChannelFlow, the open-source software due to Gibson (2010). This software is a pseudo-spectral Fourier (x) $\times$ Chebyshev (y) $\times$ Fourier (z) de-aliased scheme integrating the Navier–Stokes equations. A good compromise between computational load and realism was found by

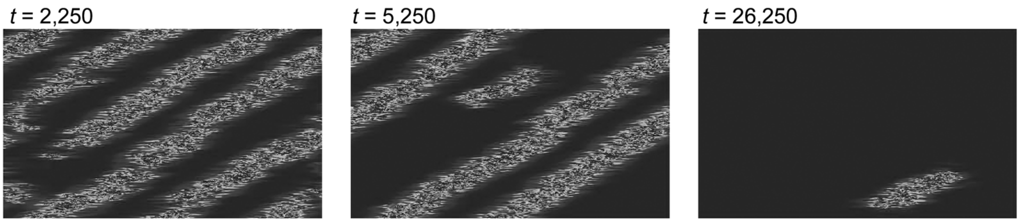

FIG. 2. Decay of bands for $R = 273.75 < R_g$ in a system of size (432×256). A laminar gap opens in a turbulent band at $t \approx 2,250$ (left); the broken band then recedes regularly (centre: illustration at $t = 5,250$). The same process next occurs on the remaining bands down to final decay (right: illustration at $t = 26,250$). Note that a band can break but recover temporarily and that the laminar gap has to be sufficiently wide for regular withdrawal to take place (see Manneville, 2011). Streamwise direction is horizontal. Colour coding of the local distance to the laminar flow: laminar is deep blue, turbulent ranges from yellow to red.

Manneville & Rolland (2010) for $N_x = L_x$ and $N_z = 3L_z$, $N_{x,z}$ being the number of collocation points used in the evaluation of in-plane dependence of non-linear terms, and $N_y = 15$, the number of Chebyshev polynomials used to describe the wall-normal dependence. This resolution may seem quite low but we showed that all the qualitative features of the transitional regime were well preserved (self-sustaining process, laminar-turbulent coexistence, and pattern selection with λ_x and λ_z comparing favourably with experimental values). The price to pay was just a moderate shift of the transitional range $[R_g, R_t]$ by $\sim$15% from $[325, 410]$ down to $[275, 360]$. On the other hand, we were able to study domains with typical domain size $L_x = 432$, $L_z = 256$ and perform many statistically significant experiments with the power of a desk-top computer only.

Within this frame, the study was focused on the vicinity of the global stability threshold R_g, considering the decay of bands at $R \lesssim R_g$, their growth from a germ (a localized patch of turbulence) at $R \gtrsim R_g$ and the existence of metastable coherent structures at steady state. It turns out that a consistent picture of what happens at the lower end R_g of the transitional range can be understood by noticing that chaos is only *transient* at the MFU scale, but that local collapse at one place can be compensated by *contamination* from neighbouring places.

2.1 *Band decay or growth*

Decay was studied in a system of size (432×256) fitting three bands in the vicinity of R_g. It appears to be controlled by two processes: (a) the formation of a laminar gap within a long enough turbulent segment and (b) a breakdown/renewal of turbulence near the segments' extremities, biased towards decay, making the segments recede regularly but only statistically; see Fig. 2 and Manneville (2011) for a detailed report.

The growth from a germ was studied in a slightly larger system of size (468×272). A typical experiment is illustrated in Fig. 3. In addition to process (b) now biased towards turbulence propagation, growth was seen to involve a third process (c): the offspring of turbulent buds near segment extremities, i.e. small turbulent patches with local orientations opposite to that of the main branch. When process (c) is sufficiently active, the pattern readily grows in a labyrinthine fashion as already observed by Duguet *et al.* (2010b). It then gets more regular by eliminating topological defects of any nature, laminar patches, dislocations and grain boundaries between well-oriented subdomains, which may take an extremely long time (a few $10^4\ h/U$); for details see Manneville (2012).

These empirical findings can quite naturally be cast into the conceptual frame put forward by Pomeau (1986) who conjectured a connection with thermodynamic *first-order phase transitions* on the

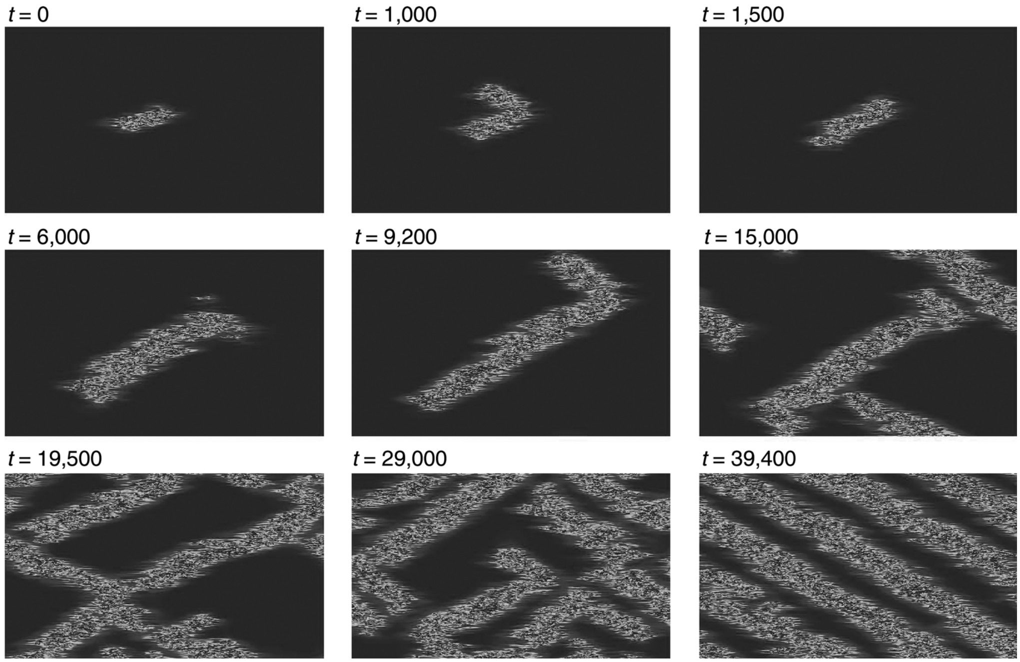

FIG. 3. Growth from a germ for $R = 285.0 > R_g$ in a system of size (468×272). From left to right and top to bottom: $t = 0$, the initial condition is an elongated and slanted turbulent patch; 'unsuccessful' branching of a turbulent bud around $t = 1,000$–$1,500$; the germ next continues to grow along its original direction after several episodes similar to what happened at $t = 1,000$, here illustration at $t = 6,000$; 'successful' branching at $t = 9{,}200$ marking the start of labyrinthine growth $t = 15,000, 19,500, 29,000$; cleaning from defects of all kinds ends in an ordered three-band pattern, here at $t = 39{,}400$. The same representation as in Fig. 2.

one hand, and *directed percolation* on the other. Crucial to a first-order transition, e.g. the liquid–gas transition, is the problem of *nucleation* of one phase inside the other, whereas directed percolation is a stochastic two-state *contamination* process governing, e.g. epidemics or forest fires (see Kinzel, 1983).

The second facet of Pomeau's proposal implies understanding the turbulent state as *active* and the laminar state as *absorbing*: Turbulence can decay to laminar flow spontaneously while the linearly stable laminar flow cannot become turbulent by itself but only under finite amplitude perturbations coming from neighbouring locations where the flow is turbulent. Depending on the local probabilities of spontaneous collapse of turbulence and contamination from neighbours, both sensitive functions of R, one will then get decay or growth at a statistical level depending on whether the system is below or above some well-defined directed percolation threshold.

On the other hand, the formation of a laminar gap or the birth of a turbulent bud are in line with the first-order character of the transition. They both result from fluctuations of the interface between the laminar flow and the turbulence. Owing to small-scale chaos at the MFU scale, these permanent fluctuations may evolve locally and temporarily into the *large deviations* producing wide indentations in a band segment, either a laminar neck evolving into a laminar gap breaking the band that next recedes at lower R, or a turbulent bud at the origin of a new differently oriented band portion at larger R.

The variation with R of probabilities of large deviations corresponding to processes (b) and (c) at the origin of decay or growth of bands is reminiscent of the findings for the pipe flow with a competition between puff decay and puff splitting pointing to the corresponding definition of R_g for that system.

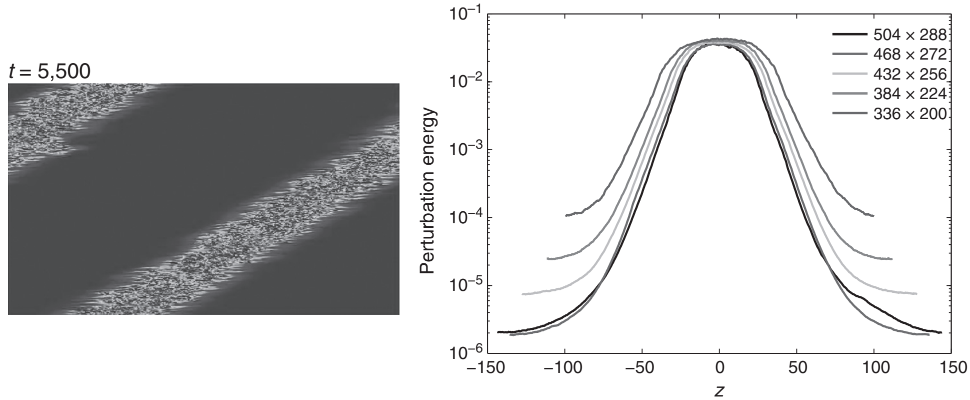

FIG. 4. Left: single steady band obtained at $R = 282.5$; domain size (432 × 256); same representation as in Fig. 2. Right: spanwise profile of the perturbation energy averaged over the diagonal of the computational domain and over 20 realizations taken every $\Delta t = 100\,h/U$ from $t = 3,500$ to $5,500\,h/U$ for each size as indicated.

For the plane Couette flow (at least as it is reproduced in our under-resolved simulations) this criterion would give $R'_{\rm g} \approx 282$ rather than $R_{\rm g} \approx 275$ as deduced from the persistence of bands down to this value.

2.2 *Solitary bands*

Whereas isolated puffs in the pipe flow do not seem to persist indefinitely but can just decay or split, as shown by Avila *et al.* (2011) and others, for the plane Couette flow seemingly sustained isolated bands have been observed by Barkley & Tuckerman (2005b) in experiments where the length of their domain was progressively increased. Their computational protocol was progressively increased but the orientation of bands fixed beforehand. We have attempted to recover these results in less restrictive conditions (though subjected to under-resolution). Such states have indeed been found in a narrow range of Reynolds numbers around $R_{\rm g}$ where band breaking is overcome by growth, so that the solitary band is expected to persist despite stronger fluctuations than in their narrow elongated oblique domain.

Systems of sizes ranging from (336 × 200) to (504 × 288), keeping the angle roughly constant ($L_z/L_x \approx 0.6$, angle $\approx 30^\circ$), have been considered at $R = 282.5$. This series was produced by taking a one-band solution in domain (468 × 272), then stretching or compressing it to fit the other sizes and next letting it reach statistical equilibrium. The particular case depicted in Fig. 4 (left) corresponds to the size (432 × 256) at $t = 5500\,h/U$. The profiles of the corresponding perturbation energy, averaged over the diagonal, are displayed in Fig. 4 (right), which strongly suggests convergence of the oblique bands towards a solitary coherent structure with well-defined shape in the large aspect-ratio limit. On the other hand, the level of perturbation increases rapidly inside the laminar region as seen when considering the size (336 × 200). For smaller sizes (namely $200 < L_x < 300$), this level is high enough to trigger the nucleation of new bands at smaller distances, ending into well-formed two-band states.

So, depending on the protocol, several different states are compatible at a given R and given size, each being locally stable, i.e. stable provided that no sufficient time is left for large deviations to nucleate a different one. The state that can naturally be obtained by decreasing R gradually, however, seems to represent an optimum into which states with fewer bands can evolve, that is three bands for $L_x \approx 400$. The existence of such an optimal wavelength at a given R resonating with the dimensions of the domain can be analysed within a Ginzburg–Landau phenomenological description of the patterning (see Rolland & Manneville, 2011).

3. Discussion

The application of pattern-formation concepts is standard in systems such as Rayleigh–Bénard convection where structures develop in a super-critical frame on a basically noiseless background (Cross & Hohenberg, 1993). A transitional plane Couette flow, in contrast, appears to be a good system to test the validity of the same approach but in a subcritical context where strong stochasticity induced by turbulence plays a crucial role.

Whereas a large body of work has been devoted to systems where coherence at the MFU scale is important, our study relates to systems in extended geometry more relevant to laboratory experiments, and for which the conceptual frame of *phase transitions* proposed by Pomeau (1986) appears most adapted. In particular, large deviations and nucleation processes inherent in first-order transitions are suggested to rule the transition to/from turbulence while directed percolation properties govern the details of growth/decay processes. Of course, it would remain to show that the appeal to controlled under-resolution in order to reach the large aspect-ratios of interest is a valid procedure. However, in view of the close correspondence between our results and experimental findings or fully resolved simulations at a moderate aspect ratio (band decay, growth from a germ, general band organization), we are confident that our computational protocol shadows the physical situation, apart from a slight shift of the relevant Reynolds number range.

The approach is thus at odds with the recent extensive use of the theory of low-dimensional dynamical systems which, on the other hand, is instrumental in interpreting the local breakdown of turbulence. It should indeed be stressed that, by enforcing periodic boundary conditions at a distance of a few h, the MFU assumption 'freezes' the flow to a temporal dynamics in a tiny portion of the phase space that exclude large-scale modulations, and widely underestimates the number of unstable directions in the phase space. This is not without consequences on the nature of the turbulent–laminar boundary and the vicinity of what we call R_{g}, where spatiotemporal chaos needs to be accounted for.

We should, however, also take care of *not* translating classical results of statistical physics and pattern formation theory too hastily. For example, it is tempting to develop a Ginzburg–Landau approach adding noise to account for the turbulence (Prigent *et al.*, 2003), which can be validated to a certain extent (Rolland & Manneville, 2011) but keeps some phenomenological flavour, while the specificity of hydrodynamic interactions may play an important role. Although this helps us understand some aspects of the pattern formation, no concrete prediction can be made on, e.g. the dependence of lifetimes of turbulent structures or other observables such as the angles and wavelengths, with the Reynolds number. Hydrodynamics and especially the generation of large-scale flows in the laminar regions by Reynolds stresses localized in the turbulent patches are indeed essential to the detailed mechanisms by which turbulent segments break down or turbulent buds branch during transient stages, or by which bands get sustained (Tuckerman & Barkley, 2011). This is of utmost importance in so far as the possible application to more general wall-bounded transitional flows is concerned.

Acknowledgments

The author would like to thank J. Rolland for his collaboration and help on computational issues, and Y. Duguet, D. Barkley, L.S. Tuckerman and the members of the Saclay Group *Instabilités et Turbulence* for many stimulating discussions.

References

Avila, K., Moxey, D., de Lozar, A., Avila, M., Barkley, D. & Hof, B. (2011) The onset of turbulence in pipe flow. *Science*, **333**, 192–196.

Barkley, D. (2011) Simplifying the complexity of pipe flow. *Phys. Rev. E*, **84**, 016309.

Barkley, D. & Tuckerman, L. S. (2005a) Computational study of turbulent laminar patterns in Couette flow. *Phys. Rev. Lett.*, **94**, DOI: 10.1103/PhysRevLett.94.14502.

Barkley, D. & Tuckerman, L. S. (2005b) Turbulent-laminar patterns in plane Couette flow. *IUTAM Symp. on Laminar-Turbulent Transition and Finite Amplitude Solutions* (T. Mullin & R.R. Kerswell eds). Springer, pp. 107–127.

Bottin, S., Daviaud, F., Manneville, P. & Dauchot, O. (1998) Discontinuous transition to spatiotemporal intermittency in plane Couette flow. *Europhys. Lett.*, **43**, 171–176.

Cross, M. C. & Hohenberg, P. C. (1993) Pattern formation outside equilibrium. *Rev. Mod. Phys.*, **65**, 851–1112.

Duguet, Y., Willis, A. P. & Kerswell R. R. (2010a) Slug genesis in cylindrical pipe flow. *J. Fluid Mech.*, **663**, 180–208.

Duguet, Y., Schlatter, Ph. & Henningson, D. S. (2010b) Formation of turbulent patterns near the onset of transition in plane Couette flow. *J. Fluid Mech.*, **650**, 119–129.

Eckhardt, B., Faisst, H., Schmiegel, A. & Schneider, T. M. (2008) Dynamical systems and the transition to turbulence in linearly stable shear flows. *Philos. Trans. R. Soc. A*, **366**, 1297–1315.

Gibson, J. F. (2010) *Channelflow: A Spectral Navier–Stokes Simulator in C++*. Available at http://www.channelflow.org/.

Gibson, J. F., Halcrow, J. & Cvitanović, P. (2009) Equilibrium and travelling-wave solutions of plane Couette flow. *J. Fluid Mech.*, **638**, 243–266.

Hamilton, J. M., Kim, J. & Waleffe F. (1995) Regeneration mechanisms of near-wall turbulence structures. *J. Fluid Mech.*, **287**, 317–348.

Jiménez, J. & Moin, P. (1991) The minimal flow unit in near wall turbulence. *J. Fluid Mech.*, **225**, 213–240.

Kinzel, W. (1983) Directed percolation. *Percolation Structures and Processes* (G. Deutscher, R. Zallen & J. Adler eds). Annals of the Israel Physical Society, vol. 5, Conference proceeding published in book form by Adam Hilger, Bristol, 1983; Kinzel's contribution is Chapter 18, pp. 425–444.

Manneville, P. (2010) *Instabilities, Chaos and Turbulence*, 2nd edn. Imperial College Press, London.

Manneville, P. (2011) On the decay of turbulence in plane Couette flow. *Fluid Dyn. Res.*, **43**, DOI:10.1088/0169-5983/43/6/065501.

Manneville, P. (2012) On the growth of laminar-turbulent patterns in plane Couette flow. *Fluid Dyn. Res.* special issue (BIFD11 conference, Barcelona July 18–21, 2011), Special issue: BIFD2011.

Manneville, P. & Rolland, J. (2010) On modelling transitional turbulent flows using under-resolved direct numerical simulations: the case of plane Couette flow. *Theor. Comput. Fluid Dyn.*, **25**, 407–420.

Philip, J. & Manneville, P. (2011) From temporal to spatiotemporal dynamics in transitional plane Couette flow. *Phys. Rev. E*, **83**, 036308 [12p].

Pomeau, Y. (1986) Front motion, metastability and subcritical bifurcations in hydrodynamics. *Physica D*, **23**, 3–11. See also Bergé, P., Pomeau, Y. & Vidal, Ch. (1998) *L'espace chaotique*, Hermann, Paris, Chapter 4 (in French).

Prigent, A. & Dauchot, O. (2005) Transition to versus from turbulence in subcritical Couette flows. *IUTAM Symp. on Laminar-Turbulent Transition and Finite Amplitude Solutions* (T. Mullin & R. R. Kerswell eds). Springer, pp. 195–219.

Prigent, A., Grégoire, G., Chaté, H. & Dauchot, O. (2003) Long-wavelength modulation of turbulent shear flows. *Physica D*, **174**, 100–113.

Rolland, J. & Manneville, P. (2011) Ginzburg–Landau description of laminar-turbulent oblique band formation in transitional plane Couette flow. *Eur. Phys. J. B*, **80**, 529–544.

Schneider, T. M., Gibson, J. F., Lagha, M., De Lillo, F. & Eckhardt, B. (2008) Laminar-turbulent boundary in plane Couette flow. *Phys. Rev. E*, **78**, 037301.

Tuckerman, L. S. & Barkley, D. (2011) Patterns and dynamics in transitional plane Couette flow. *Phys. Fluids*, **23**, 041301 [9p].

Waleffe, F. (2003) Homotopy of exact coherent structures in plane shear flows. *Phys. Fluids*, **15**, 1517–1534.